Talanta 210 (2020) 120642

Contents lists available at ScienceDirect

Talanta

journal homepage: www.elsevier.com/locate/talanta

Carboxymethyl-botryosphaeran stabilized carbon nanotubes aqueous dispersion: A new platform design for electrochemical sensing of desloratadine

Carlos A.R. Salamanca-Neto[a,*], André Olean-Oliveira[b], Jessica Scremin[a], Graziela S. Ceravolo[c], Robert F.H. Dekker[d], Aneli M. Barbosa-Dekker[e], Marcos F.S. Teixeira[b], Elen R. Sartori[a,*]

[a] Laboratório de Eletroanalítica e Sensores, Departamento de Química, Centro de Ciências Exatas, Universidade Estadual de Londrina, CEP, 86057-970, Londrina, PR, Brazil
[b] Departamento de Química e Bioquímica, Faculdade de Ciências e Tecnologia, Universidade Estadual Paulista (UNESP), Presidente Prudente, SP, Brazil
[c] Departamento de Fisiologia, Centro de Ciências Biológicas, Universidade Estadual de Londrina, Londrina, PR, 86057-970, Brazil
[d] Programa de Pós-Graduação em Engenharia Ambiental, Universidade Tecnológica Federal do Paraná, Câmpus Londrina, CEP, 86036-370, Londrina, PR, Brazil
[e] Departamento de Química, Centro de Ciências Exatas, Universidade Estadual de Londrina, CEP, 86057-970, Londrina, PR, Brazil

ARTICLE INFO

Keywords:
Botryosphaeria rhodina MAMB-05
MWCNTs aqueous dispersion
Modified glassy carbon electrode
Pharmaceutical analysis
Biological sample

ABSTRACT

The polysaccharide carboxymethyl-botryosphaeran (CMB) was used to improve the dispersion of multi-walled carbon nanotubes (MWCNTs) in water. This feature was applied in modifying a glassy carbon electrode (GCE) to construct a sensitive voltammetric sensor for the determination of desloratadine (DESL), a tricyclic antihistamine. The morphology and spectroscopic behavior of the sensor were evaluated. The modified sensor was characterized as homogeneous, and presented a higher electroactive area and a lower charge transfer resistance compared to the unmodified GCE. Using linear sweep voltammetry at 25 mV s^{-1}, the developed sensor presented a sensitivity of 1.018 μA L μmol^{-1} in the linear working range of 1.99–32.9 μmol L^{-1}, with a detection limit of 0.88 μmol L^{-1} of DESL in 0.10 mol L^{-1} potassium hydrogen-phosphate solution (pH 8.0). In addition, the sensor showed excellent repeatability with a relative standard deviation of only 1.02% for a sequence of 10 measurements. The sensor was successfully applied in the analysis of pharmaceutical preparations containing DESL, with equivalent results compared to a validated spectrophotometric method at the 95% confidence level. The sensor was also employed in the analysis of a spiked sample of DESL in rat serum.

1. Introduction

Desloratadine (DESL, 8-chloro-6,11-dihydro-11-(4-piperdinylidene)-5*H*-benzo [5,6]cyclohapta [1,2-b]pyridine, Fig. S1 – supplementary material) is a third-generation selective antihistaminic drug that functions as a H_1-antagonist of histamine on cell receptor sites, and is used to treat allergic symptoms without causing sedation.

Several analytical methods have been reported in the literature describing the determination of DESL in pharmaceutical preparations. These methods are generally based upon spectrophotometry [1,2] and chromatography [3,4], but electrochemical analysis has also been used [5,6]. Chromatography is the preferred method since it allows the determination of DESL simultaneously with other analytes present in complex matrices. Chromatographic instrumentation, however, is relatively expensive and requires the use of costly high purity solvents, besides presenting long times for sample preparation and analysis. In this sense, the use of low-cost, rapid and technical easy-to-handle methods is preferred.

In the past decade, many electroanalytical methods had been developed for a large variety of analytes [7–11]. These methods are generally cheaper using low-cost materials, are faster and easier to operate, and are considered environmentally-friendly. The electroanalytical procedures are mainly based upon the interaction of the analyte with the surface of an electrode. With the development of new materials, especially nanostructured materials, several designs of working electrodes can be assembled by a simple modification of those traditionally employed to fabricate chemically-modified electrodes [8,12–14].

The main reason to modify an electrode is to promote electrocatalysis, i.e., to increase the analytical signal, and/or to shift the redox potential in order to allow the analyte to oxidize/reduce within the working potential range of the particular electrode [14,15]. Multi-

* Corresponding authors.
E-mail addresses: carlos.salamanca@uel.br (C.A.R. Salamanca-Neto), elensartori@uel.br (E.R. Sartori).

https://doi.org/10.1016/j.talanta.2019.120642
Received 2 October 2019; Received in revised form 8 December 2019; Accepted 9 December 2019
Available online 16 December 2019
0039-9140/

walled carbon nanotubes (MWCNTs) have extensively been used to modify electrodes since, as a nanostructured material, present electrocatalytic features due to their high surface area and electron mobility [16–18].

The procedure of preparing and using MWCNTs as an electrode modifier is based upon their suspension/dispersion in a specific solvent before drop casting onto the electrode surface. This step has been described in many papers, and some examples of treating and dispersing MWCNTs in solvents are presented in Table S1 (supplementary material). Most of the procedures make use of acid media to treat MWCNTs in order to facilitate their dispersion in polar solvents due to the carboxyl groups generated. When pristine, the MWCNTs could be dispersed in organic solvent such as methanol [19], and in an aqueous solution of β-cyclodextrin (cyclic oligosaccharides containing 7 glucose residues linked by α-(1 → 4)-bonds forming cage-like structures) [20]. Recently, polysaccharides were discovered that increase the water dispersive capability of carbon nanostructures [21], and the dispersion of MWCNTs in aqueous media was made possible by different substrates acting as dispersants, such as chitosan and β-cyclodextrin [20,22–24].

In this sense, the fungal exopolysaccharide named botryosphaeran, a β-glucan of the (1 → 3)(1 → 6)-β-D-glucan type from *Botryosphaeria rhodina* MAMB-05 [25] derivatized chemically by carboxymethylation to produce carboxymethyl-botryosphaeran (CMB), was considered, as recently it was demonstrated to possess new electroanalytical applications [26]. CMB has not been used for the purpose of dispersing MWCNTs. Thus, in this work, we propose, and report on the use of CMB to disperse MWCNTs in water to facilitate easy construction of an electrochemical sensor for the measurement of the antihistamine drug, DESL.

2. Experimental

2.1. Chemicals and solutions

All chemicals used in this work were of analytical grade and used as received, and all the solutions were prepared using ultra-purified water (resistivity ≥ 18.2 MΩ cm) obtained from a Milli-Q system (Millipore, USA).

DESL standard (99.8%) and MWCNTs (20–30 nm in diameter and 0.5–2 μm in length; purity: ≥ 95%) was obtained from Sigma-Aldrich (St Louis, MO, USA). The pharmaceutical preparations containing DESL were purchased from a local pharmacy in Londrina, Brazil.

The supporting electrolyte of voltammetric measurements was a 0.10 mol L^{-1} potassium hydrogen-phosphate solution with the pH adjusted to 8.0 with 2.0 mol L^{-1} NaOH. DESL stock solutions of 10 mmol L^{-1} were freshly prepared by dissolving the standard in ultrapure water. Working solutions were prepared by dilution of the stock solution with the supporting electrolyte.

2.2. Apparatus

All voltammetric measurements were carried out using a PGSTAT 101 potentiostat/galvanostat (Metrohm Autolab B. V., Schiedam, Netherlands) controlled by NOVA 2.1 software. A conventional three-electrode glass cell was employed, using a platinum plate as the auxiliary electrode, Ag/AgCl (3.0 mol L^{-1} KCl) as the reference electrode, and the developed sensor as the working electrode. The glassy carbon electrode (GCE) was obtained from Tokay Carbon Co., Tokyo, Japan (5 mm, diameter).

The electrochemical impedance spectroscopy (EIS) experiments were carried out using a FRA II μAutolab type III potentiostat/galvanostat (Metrohm Autolab B. V., Schiedam, Netherlands) controlled by NOVA 1.0 software. The experiments were performed at the formal potential of the $[Fe(CN)_6]^{3-/4-}$ redox pair (0.27 V for the electrodes employed in this work), ranging from 10 mHz to 100 KHz (10 points per decade), and with a 10 mV (rms) ac perturbation. The solution consisted of 5.0 mmol L^{-1} $K_3[Fe(CN)_6]$, 5.0 mmol L^{-1} $K_4[Fe(CN)_6]$ and 0.5 mol L^{-1} KCl.

The pH of solutions was measured using a pH meter (Hanna® Instruments Brasil, Barueri, Brazil), model HI-221, employing a combined glass electrode with an Ag/AgCl (3.0 mol L^{-1} KCl) external reference electrode.

Microscopy images were obtained using a scanning electron microscope (SEM, model FEI Quanta 200, Thermo Fisher Scientific, Waltham, MA, USA) operated at 5000 V.

2.3. Production of carboxymethyl-botryosphaeran and the preparation of the modified electrode

Botryosphaeran was obtained from the ascomyceteous fungus *Botryosphaeria rhodina* MAMB-05 grown by submerged fermentation on nutrient medium containing 50 g mL^{-1} sucrose according to Barbosa et al. [27], and its carboxymethylation was performed according to the method outlined by Xu et al. [28] with modifications as described by Eisele et al. (2019). The degree of substitution (DS) of carboxymethyl groups on botryosphaeran used in this work was 0.84.

Prior to modification, the GCE was carefully polished with slurries of 0.05 μm alumina followed by rinsing with ultra-pure water, and then allowed to dry at room temperature during 10 min.

An aqueous dispersion of the MWCNTs was prepared by mixing 5.0 mg of pristine MWCNTs in 5 mL of an aqueous solution containing 1 mg mL^{-1} of CMB, followed by sonication in an ultrasound bath for 5 min. The CMB-MWCNTs dispersion was stored under refrigeration. Prior to modification of the GCE, the dispersion was kept in an ultrasound bath for 1 min.

The sensor was prepared by the single-drop casting method. The previously alumina-polished GCE was placed in the vertical position, and then 20 μL of the aqueous dispersion of MWCNTs was dropped onto the electrode surface with the aid of a micropipette, and allowed to dry at room temperature. The sensor prepared is denoted as CMB-MWCNTs/GCE. The sensor was activated in potassium hydrogen-phosphate solution (pH 8.0) by applying ten cycles in a potential window from 0.0 to 1.4 V at a scan rate 100 mV s^{-1} using cyclic voltammetry (CV). Two other sensors were also prepared by the drop (20 μL) casting method for comparative purposes: MWCNTs/GCE – 1 mg mL^{-1} suspension of MWNCTs in water, and CMB/GCE – 1 mg mL^{-1} aqueous solution of CMB.

2.4. General analytical procedures and sample preparation

Linear sweep voltammetry (LSV) was employed for the construction of the analytical curves for DESL determination. The detection limit (LOD) values were calculated using the formula: $3s/m$, where s is the standard deviation of intercept of the analytical curve, and m is the slope of the analytical curve [29]. The statistical parameters were obtained using Origin Pro 8 software at the significance level of 5%.

The pharmaceutical preparations containing DESL used were tablets (Biosintética, São Paulo, Brazil) labeled 5 mg $tablet^{-1}$, and oral solutions (ESALERG – Aché, Guarulhos, Brazil) labeled 0.5 mg mL^{-1}. The preparation of the tablet samples for analysis was performed as follow. Ten tablets of each preparation were finely powdered in a mortar and pestle and an aliquot representative of one single tablet (5 mg of DESL) was transferred into a 10 mL volumetric flask, and the volume completed with potassium hydrogen-phosphate solution (pH 8.0) and sonicated in an ultrasound bath at room temperature for 5 min. The oral solution samples were directly analyzed, no prior preparation or dilution.

For the voltammetric analyses, an aliquot of the DESL tablets solutions, as well as an aliquot of the oral solutions, were directly transferred to the electrochemical cell containing 10 mL of the supporting electrolyte. To ensure significance of the results, measurements were performed in triplicate. The DESL concentration in each sample was

determined by using the previously obtained analytical curve. For comparative purposes, the pharmaceutical preparations were also analyzed using a validated spectrophotometric method [2].

The sensor performance was also evaluated on a sample of rat blood serum spiked with DESL. The blood sample was obtained from a female rat from the breeding stock of the Centro de Ciências Biológicas of the Universidade Estadual de Londrina. The rat was maintained in a temperature-controlled room on a 12-h light/dark cycle, with standard rat ration (Nuvital, Curitiba, Brazil) and water *ad libitum*. At 12 weeks of age, the rat was anesthetized (sodium thiopental, 40 mg kg^{-1}; i.p.), a blood sample was collected from the abdominal aorta and then centrifuged to separate the serum which was used in the experiments. The blood sample collection procedure was approved by the Ethics Committee for Animal Research (CEUA/UEL: 6996.2015.02) at Universidade Estadual de Londrina-PR, Brazil.

3. Results and discussion

3.1. Dispersion of MWCNTs in CMB and the construction of the electrodes

The dispersion of the MWCNTs was assessed by mixing 5.0 mg of the carbonaceous nanomaterial with (i) 5 mL of water, and in separate experiments, (ii) 5.0 mg of lyophilized underivatized botryosphaeran in 5 mL of water, and (iii) 5 mL of an aqueous solution of CMB. All mixtures were sonicated for 5 min in an ultrasound bath at room temperature. Fig. S2 (supplementary material) presents photographs of the resulting dispersions obtained. As shown, the MWCNTs did not disperse readily in water because the carbon nanomaterial tended to aggregate [24]. When botryosphaeran was added, the carbon nanotubes still aggregated, however, the addition of CMB to the MWCNTs-water mixture promoted the complete dispersion of the MWCNTs. This occurred because the polar biomolecules of CMB containing carboxymethyl groups have high affinity for carbon-containing structures enabling the pristine MWCNTs to be homogeneously distributed in a water solution [21,30–33]. The effect of addition of CMB to disperse pristine MWCNTs was verified.

Following this step, three different electrodes were prepared by modifying the bare GCE. They included GCE modified with (i) CMB (CMB/GCE), (ii) MWCNTs-suspension in water (MWCNTs/GCE), and (iii) CMB-stabilized MWCNTs aqueous dispersion (CMB-MWCNTs/GCE), and were used for comparison purposes.

3.2. Morphological characterization of the prepared electrodes

SEM images of the CMB-MWCNTs/GCE and the other prepared electrodes (as described above) are shown in Fig. 1. In Fig. 1A, the CMB molecules were found to cover parts of the GCE clear surface. In the MWCNTs/GCE electrode, SEM imaging indicated that the MWCNTs did not distribute well on the GCE surface using the MWCNTs-water suspension (Fig. 1B). SEM imaging of the CMB-stabilized MWCNTs aqueous dispersion on the electrode is shown in Fig. 1C, indicating a homogeneous distribution of the dispersed nanomaterial. It was possible to observe that CMB coated the MWCNTs as its thickness increased.

The electroactive area of the fabricated electrodes was obtained by cyclic voltammetric measurements using 5.0 mmol L^{-1} $K_3[Fe(CN)_6]$ in 0.10 mol L^{-1} KCl at different scan rates. The slope values from the current *vs* $v^{1/2}$ plots were employed in the Randles-Sevcik equation [34]. The electroactive area of GCE and each of the modified electrodes is presented in Table S2 (supplementary material). The results demonstrated that the use of carbon nanomaterial in the GCE modification (MWCNTs/GCE) led to an increase in the electroactive area compared to the unmodified GCE, while the use of CMB (CMB/GCE) decreased the electroactive area. Furthermore, the surface of the electrode was not completely covered by the nanomaterial when using the suspension of the MWCNTs in water (MWCNTs/GCE – Fig. 1B) in the absence of CMB. CMB stabilized the aqueous dispersion of MWCNTs for the modification of GCE and exhibited the highest electroactive area. It is important to note that even with the non-conductive properties of CMB, the homogeneity of the modifier was responsible for the equal distribution of the nanomaterial on the surface of the GCE (Fig. 1C) leading to the highest electroactive area obtained by the CMB-MWCNTs/GCE.

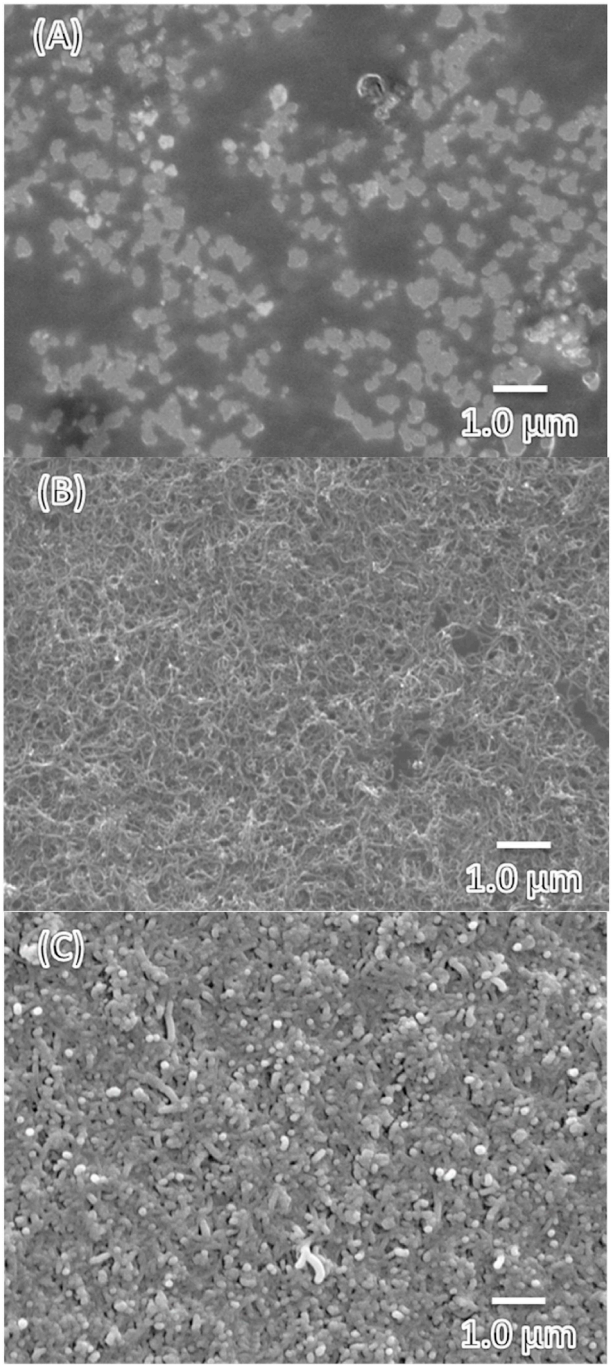

Fig. 1. SEM images of the following modified glassy carbon electrodes: (A) CMB/GCE, (B) MWCNTs/GCE, and (C) CMB-MWCNTs/GCE.

3.3. Spectroscopic study of the interfacial properties of the prepared electrodes

EIS measurements were made to characterize the electrodes in the $[Fe(CN)_6]^{3-/4-}$ probe solution to monitor the electron transfer

resistance (R_{ct}) value. This was obtained from the semicircle formed in the region of high frequency after subtraction of the resistance value of the solution [35–37]. Fig. S3 (supplementary material) shows the spectra of GCE and the modified electrodes CMB/GCE, MWCNTs/GCE and CMB-MWCNTs/GCE in 0.01 mol L^{-1} solution of $[Fe(CN)_6]^{3-/4-}$, in the frequency range of 100 KHz to 0.1 Hz, under the applied potential of 0.27 V vs Ag/AgCl. Table S2 (supplementary material) also showed that there was an increase of 60 Ω when the GCE was modified with CMB, compared to the bare GCE. In the presence of the MWCNTs in the composite matrix, there was a significant decrease in the value of R_{ct}, from 149.7 Ω (CMB/GCE) to 3.6 Ω (CMB-MWCNTs/GCE); a decrease of about 98% in the value of R_{ct} because of the presence of MWCNTs.

The heterogeneous rate constants (K_{app}) of the electrodes were calculated for comparative purposes (Table S2, supplementary material). The constant revealed the kinetic rate at which the reaction between the probe species and the electrode moved towards equilibrium [38]. K_{app} was calculated for the electrodes from the equation:

$$K_{app} = \frac{RT}{F^2 R_{ct} AC}$$

where K_{app} is the standard heterogeneous electron transfer rate constant (cm s^{-1}), R the universal gas constant (8.314 J K^{-1} mol^{-1}), T the thermodynamic temperature (298.15 K), F the Faraday constant (96,485 C mol^{-1}), R_{ct} the electron transfer resistance (Ω), A the electrode active area (cm^2), and C the concentration of the $[Fe(CN)_6]^{3-/4-}$ solution (10 μmol cm^{-3}).

The results of K_{app} (Table S2, supplementary material) revealed faster electron transfer to the electrodes containing MWCNTs confirming the electrocatalytic features of this nanomaterial. On the other hand, comparing the electrodes with and without added CMB, it was possible to observe that the presence of this biopolymer molecule caused a decrease in the electron transfer rate, as previously reported [26], indicating its insulating properties.

EIS was also applied to investigate the interfacial properties of the prepared electrodes in potassium hydrogen-phosphate solution (pH 8.0) in the absence and presence of 99.0 μmol L^{-1} of DESL (Fig. 2). The applied potential of 1.10 V was chosen according to the oxidation peak of DESL as found in the cyclic voltammograms for the modified glassy carbon electrodes in the presence of the analyte DESL. The analysis of the Nyquist complex plane spectra was performed using equivalent circuit models and the elements' values were obtained by mathematical adjustments based upon these models. The results are presented in Table 1. The GCE and CMB/GCE electrodes presented a circuit model equivalent based on the adsorption model $R(R\ \mathrm{CPE}(R\ \mathrm{CPE}))$ [39]. The circuit was in accordance with previous studies for carbon-based electrodes coated and uncoated with Nafion® [40,41]. The alterations for the correction of the adsorption of OH species onto the surface of the electrode was made due to the applied potential and the presence of oxygen in the medium [42,43]. The model contained a solution resistance R_{Ω}, a charge transfer resistance associated with the electrode/solution interface R_{ct}, and an adsorption resistance R_{ad}. The two constant phase elements (CPE) are associated with double layer capacitance (CPE_{dl}) and adsorption capacitance (CPE_{ad}). The presence of CMB covering the surface of the CGE decreased the value of R_{ct}, and increased the value of R_{ad}, due to the presence of the polysaccharide on the surface of the electrode. In the presence of 99.0 μmol L^{-1} of DESL, both electrodes presented increases in the value of R_{ct}, demonstrating a non-catalytic behavior of CMB in the presence of DESL.

For the electrodes MWCNTs/GCE and CMB-MWCNTs/GCE, the equivalent circuit model used was based on the $R(R\ \mathrm{CPE})(R\ \mathrm{CPE})$ interface model, containing a solution resistance R_{Ω} in series with two parallels. The high-medium frequency parallel containing a charge transfer resistance is associated with the material/solution interface (R_{ct}) in parallel with a double layer capacitance (CPE_{dl}). The parallel of medium-low frequency regions containing a charge transfer resistance for the film/electrode interface (R_{ct2}) in parallel to a film capacitance (CPE_{film}) is characteristic of surfaces coated with MWCNTs [45]. The addition of MWCNTs in the electrodes decreased the impedance values of the system as observed in Fig. 2, as well as a dramatic decrease in the R_{ct} values, since it is well known that MWCNTs have excellent conductive properties [46]. The results revealed that both electrodes containing MWCNTs exhibited similar values of their elements, with a small decrease in R_{ct} for the electrode containing CMB (1.24 kΩ cm^2) compared to the electrode that used only water as the dispersant (2.04 kΩ cm^2), demonstrating that CMB improved the distribution of the MWCNTs on the surface of the electrode. In the presence of DESL, both electrodes presented a decrease in their R_{ct} values, however, the electrode containing CMB had a higher ΔR_{ct} compared to the MWCNTs/GCE electrode; 510 and 300 Ω cm^2, respectively. The increase in the electrode performance can be associated with a better distribution of the MWCNTs onto the electrode surface due to the presence of CMB. A decrease in the value of R_{ct2} for the CMB-MWCNTs/GCE electrode was also observed in contrast to the increase in R_{ct2} for the MWCNTs/GCE electrode, demonstrating an improvement in film/electrode interface transfer.

3.4. Electrochemical performance of the prepared electrodes for sensing DESL

The electrochemical behavior of DESL was assessed using the different modifications of GCE. Conditions employed were CV (50 mV s^{-1}) and DESL 99.0 μmol L^{-1} in potassium hydrogen-phosphate solution (pH 8.0). Cyclic voltammetric profiles of DESL were obtained for bare GCE, CMB/CGE, MWCNTs/GCE and CMB-MWCNTs/CGE and the responses obtained are shown in Fig. 3. As can be observed, DESL did not present electrochemical responses on bare GCE and CMB/CGE under the conditions employed. An irreversible peak for DESL oxidation was observed at around 1.17 and 1.08 V when using MWCNTs/GCE and CMB-MWCNTs/GCE, respectively. A more positive oxidation potential of DESL on MWCNTs/GCE resulted from a partially exposed GCE surface, as can be observed in Fig. 1B. This behavior highlighted the electrocatalytic performance of the MWCNTs in electroanalysis.

In order to assess the reproducibility of the electrode preparations (MWCNTs/GCE and CMB-MWCNTs/GCE), each suspension/dispersion was used to prepare three electrodes, and cyclic voltammetric analyses of DESL were performed using them. The electrochemical behavior of DESL on the MWCNTs/GCE was characterized by a very unstable current of 102 ± 12.7 μA, as the reproducibility of the electrode preparation was very poor because of the MWCNTs' lower dispersion capability in water. With the stabilization of MWNCTs dispersion in water by the addition of CMB, the reproducibility of the electrode preparation (CMB-MWCNTs/CGE) could be improved, and the electrochemical response of DESL became more stable with a current of 97.6 ± 1.1 μA. It is important to mention that the addition of CMB to the electrode led to a reduction in the DESL current that was due to the non-conducting properties of polysaccharides [47]. The advantage of the reproducibility of the measurements was the major contribution of CMB in the construction of the electrode for DESL analysis.

The amount of MWCNTs and CMB as a function of its dispersion was also examined. The ratios were 1:1, 2:1 and 1:2 (mg mL^{-1}:mg mL^{-1}; MWCNTs:CMB). A ratio of 2:1 was not sufficient to obtain a homogeneous dispersion because there was insufficient biomolecules to wrap around the carbon nanostructures. Moreover, as observed in Fig. 3, the addition of CMB led to a slight decrease in the DESL current. Considering this fact, a ratio of 1:1 was chosen for use in the analysis guaranteeing a homogeneous dispersion, reproducible electrode preparation, and a relatively higher and stable DESL analytical response.

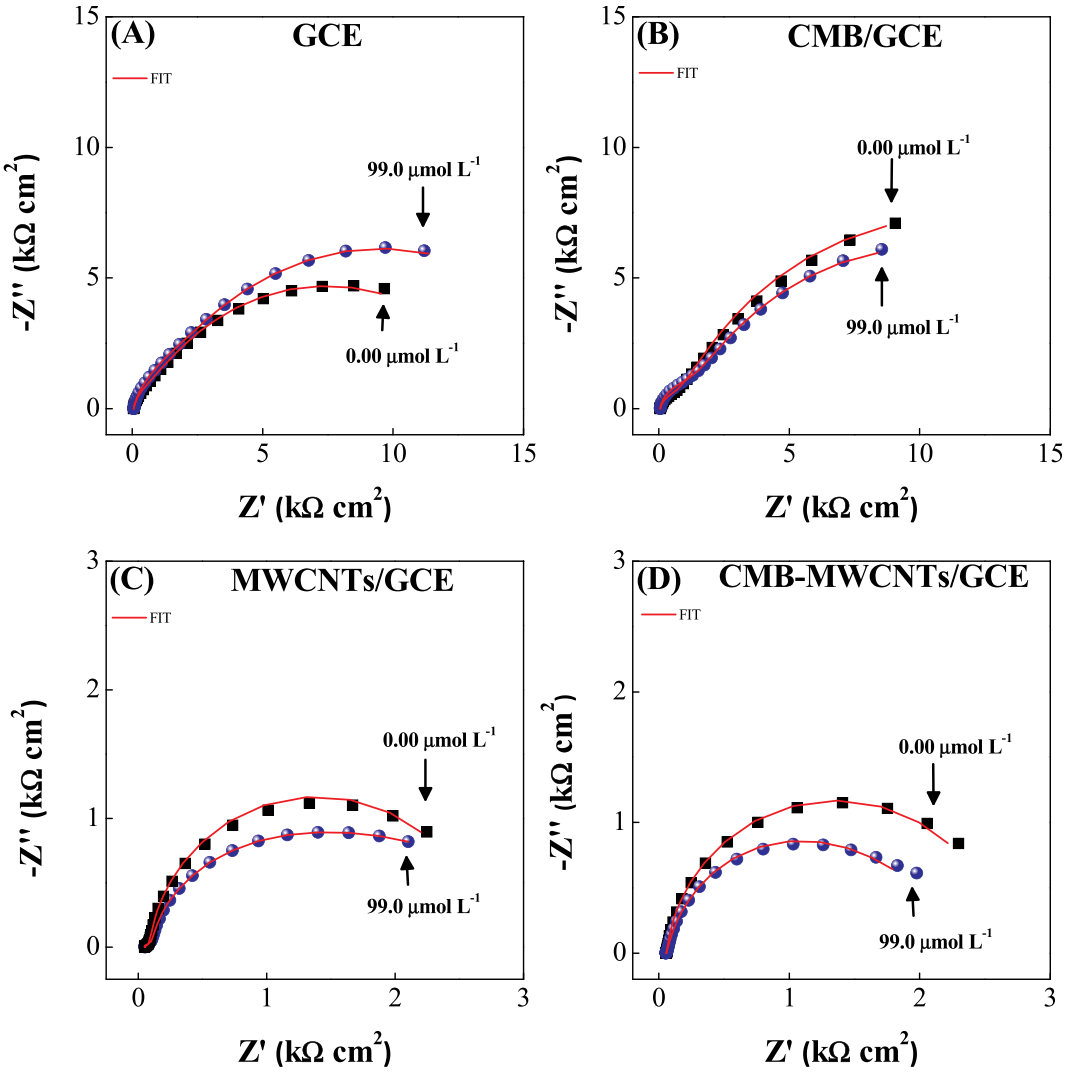

Fig. 2. Nyquist diagrams of GCE (A), CMB/GCE (B), MWCNTs/GCE (C) and CMB-MWCNTs/GCE (D) in potassium hydrogen-phosphate solution (pH 8.0) in the presence and absence of 99.0 µmol L^{-1} DESL. $E_{applied}$ = 1.10 V.

Table 1
Parameters determined from the fitting of the electrochemical impedance spectra in Fig. 2 in the absence and presence of DESL (99.0 µmol L^{-1}) using GCE, CMB/GCE, MWCNTs/GCE and CMB-MWCNTs/GCE.

Interface	DESL (µmol L^{-1})	R_{ct} (KΩ cm^2)	R_{ad} (KΩ cm^2)	CPE_{dl} (µF cm^{-2} $s^{\alpha-1}$)	α_{dl}[a]	CPE_{film} (µF cm^{-2} $s^{\alpha-1}$)	α_{film}[a]	Equivalent circuit
GCE	0.00	2.04	12.4	23.9	0.89	62.7	0.71	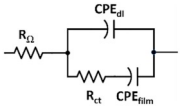
	99.0	4.47	13.4	29.0	0.88	62.4	0.77	
CMB/GCE	0.00	1.24	20.6	19.9	0.86	87.3	0.73	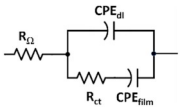
	99.0	1.85	17.7	17.9	0.91	103	0.72	
MWCNTs/GCE	0.00	2.61	0.04	28.9	0.92	390	0.60	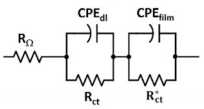
	99.0	2.31	0.05	23.9	0.86	266	0.64	
CMB-MWCNTs/GCE	0.00	2.59	0.05	26.8	0.93	500	0.62	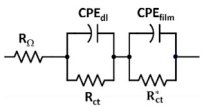
	99.0	2.08	0.01	22.0	0.88	498	0.65	

$E_{applied}$ = 1.10 V vs. Ag/AgCl. R_{Ω} = 22 Ω cm^2. The fitting error is ≤ 2%.
[a] α_{dl} and α_{film} are CPE coefficients that represent the degree of distancing for an ideal capacitor [44].

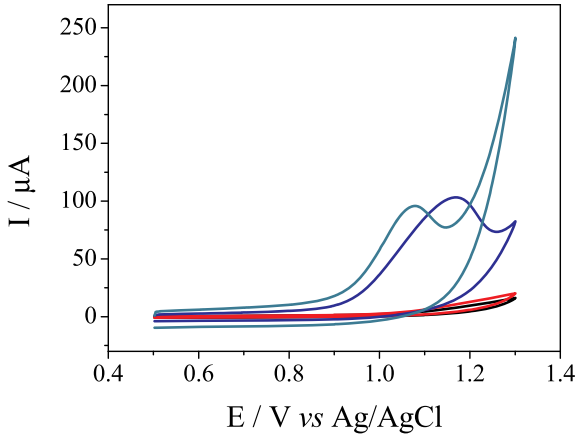

Fig. 3. Cyclic voltammograms (50 mV s^{-1}) of DESL 99.0 μmol L^{-1} in potassium hydrogen-phosphate solution (pH 8.0) for bare GCE (−), CMB/CGE (−), MWCNTs/GCE (−) and CMB-MWCNTs/CGE (−).

3.5. The effect of pH and scan rate on DESL response

The influence of pH on the electrooxidation of DESL on CMB-MWCNTs/CGE was examined using potassium hydrogen-phosphate solution with the pH adjusted in the pH range of 2.0–10.0, and CV (50 mV s^{-1}). DESL did not present oxidation responses at pH lower than 6.0 under these experimental conditions. Fig. S4 (supplementary material) shows the cyclic voltammograms obtained for 99.0 μmol L^{-1} DESL in the pH range of 6.0–10.0 using the CMB-MWCNTs/GCE. As can be seen, DESL presented well-resolved oxidation peaks at these pH values, and DESL presented highest current response at pH 8.0. This pH value was therefore selected for further analyses. In addition, the relationship between pH and oxidation potential resulted in a linear dependence (R^2 = 0.998) with slope (−66.2 mV pH^{-1}) close to the Nernstian value (−59.2 mV pH^{-1}) indicating that DESL underwent electrooxidation losing equal numbers of protons and electrons.

The number of electrons (n) was estimated by using the cyclic voltammogram obtained at pH 8.0, and equation $E_p - E_{p/2} = 47.7\ mV/\alpha n$ [34]. The following values were observed: E_p was 1.07 V and $E_{p/2}$ 0.982 V, and considering α = 0.5 (average value for irreversible systems [34]), the number of electrons was found as 1. Considering the energy levels of the molecular orbitals of DESL [48], the oxidation is thought to occur in the pyridine ring by losing one electron and one proton.

Cyclic voltammograms for DESL 99.0 μmol L^{-1} in potassium hydrogen-phosphate solution (pH 8.0) on the CMB-MWCNTs/GCE were obtained at different scan rates (5–200 mV s^{-1}). The E_p was found to shift to more positive potentials by increasing the scan rate (data not shown), confirming the irreversibility of the electrochemical reaction [34,49]. In addition, a linear relationship (R^2 = 0.990) was obtained between the logarithm of scan rate and the logarithm of current, with a slope value of 0.74 indicating that the electrochemical reaction was controlled by a mix of diffusion and adsorption of DESL towards/onto the surface of the CMB-MWCNTs/GCE [34,49].

3.6. Analytical curves for DESL on the CMB-MWCNTs/CGE

Linear sweep voltammetry (LSV) at different scan rates was employed to construct the analytical curves on the CMB-MWCNTs/CGE in order to determine the lowest concentration of DESL and the highest sensitivity with statistical confidence. Table 2 presents the analytical parameters of the curves obtained using different scan rates as well as the statistical parameters obtained for regression analysis at the 95% confidence level. Considering the critical value of F (4.49) and p (0.05), the analytical curves proved to present linear behavior. At the higher scan rate, a lower LOD and higher detectability and sensitivity were observed, but this was accompanied by a higher relative standard deviation between the measurements. Thus, based on the repeatability (lowest RSD) of the analytical response, the scan rate of 25 mV s^{-1} was chosen for the analysis of DESL by the CMB-MWCNTs/CGE, and the corresponding analytical equation is given by $I_{DESL}/\mu A = -1.33 + 1.018\ [DESL]/\mu mol\ L^{-1}$, R^2 = 0.997.

Additionally, the analytical parameters obtained with the use of the CMB-MWCNTs/GCE and LSV procedure compared with other electrodes and voltammetric techniques previously published to determine DESL are presented in Table S3 (supplementary material). As CMB-MWCNTs/GCE consisted of a modified electrode, some steps for its preparation were required. However, the LSV method proposed in our work has some advantages over the other procedures published, as it did not require preparation steps, such as deaeration and pre-concentration time, and presented excellent repeatability over a wider linear range with a relative low limit of detection.

3.7. Precision

The precision of DESL measurements by the CMB-MWCNTs/CGE was evaluated in terms of repeatability and intermediate precision. The repeatability was assessed by means of the relative standard deviation (RSD) of ten measurements using a concentration of DESL of 4.98 μmol L^{-1}. As presented in Table 2, the RSD obtained was 1.02%. The intermediate precision of DESL responses was assessed by measuring DESL at 4.98 μmol L^{-1} over five different days over a 2-week period using the same electrode, and was compared to a freshly-prepared electrode on each day of the assessment. In terms of RSD, a value of 3.49% was obtained when DESL was analyzed by the same electrode, and 4.88% using the freshly prepared electrodes. This procedure determined the precision of DESL analysis by LSV employing the CMB-MWCNTs/GCE and confirmed the storage capability of this newly constructed electrochemical sensoring device.

3.8. Selectivity

The selectivity of the electrode (CMB-MWCNTs/CGE) was examined by LSV (25 mV s^{-1}) using 4.98 μmol L^{-1} DESL in the absence and presence of possible interfering agents within the same concentration of analyte (4.98 μmol L^{-1}) in the volume ratio of 1:1, and at higher concentrations (49.5 μmol L^{-1}, ratio 1:10). The voltammograms obtained for 4.98 μmol L^{-1} DESL in the absence and presence of 49.5 μmol L^{-1} concentrations of ascorbic acid (AA), dopamine (DOP), glucose, uric acid (UA), and urea, revealed that AA, glucose and urea

Table 2
Analytical and statistical parameters of DESL analytical curves obtained with CMB-MWCNTs/CGE at different scan rates using linear sweep voltammetry.

Scan rate (mV s^{-1})	Range of concentration (μmol L^{-1})	LOD (μmol L^{-1})	Sensitivity (μA L μmol^{-1})	R^2_{adj}	F_{reg}	p value	Repeatability[a] (RSD %)
10	2.99–32.9	1.44	0.3575	0.993	826.4	< 0.001	1.88
25	1.49–32.9	0.88	1.018	0.997	3389	< 0.001	1.02
50	1.49–22.5	0.57	1.112	0.991	661.6	< 0.001	4.19
75	0.99–15.8	0.43	1.162	0.985	318.9	< 0.001	4.95

[a] n = 10; DESL concentration = 4.98 μmol L^{-1}.

Table 3
Results obtained for the analysis of the DESL content in commercial pharmaceutical tablets in potassium hydrogen-phosphate solution (pH 8.0) by the linear sweep voltammetric method and CMB-MWCNTs/CGE, compared to those obtained by the validated spectrophotometric method.

Sample	DESL content[a]			Relative Error (E_r, %)[b]	F_{calc}
	Label	LSV	Spectrophotometry		
Tablet A	5 mg cpmd^{-1}	4.80 ± 0.14	4.63 ± 0.31	3.67	4.90
Tablet B	5 mg cpmd^{-1}	5.01 ± 0.21	4.92 ± 0.40	1.83	3.63
Oral solution A	0.5 mg mL^{-1}	0.477 ± 0.08	0.487 ± 0.15	−2.05	3.52
Oral solution B	0.5 mg mL^{-1}	0.494 ± 0.09	0.475 ± 0.11	4.00	1.49

[a] Performed in triplicate; units according to the label.
[b] E_r = 100% x ([LSV – Spectroscopy value]/[Spectroscopy value]).

were found to be electroinactive in the tested potential window (0–1.4 V), and that DOP and UA presented oxidation peaks in potentials different of the DESL potential. Their interference was monitored in terms of the relative response (%) of DESL when the interfering agent was added (Table S4; supplementary material). As can be observed, the DESL response presented a maximum variation of 7.5% in presence of UA at ten times more concentrated. These results indicated the potential of the modified sensor to determine DESL in biological fluids, as none of the interfering agents presented oxidation peaks at the DESL potential, and the DESL current was observed not to change significantly in the presence of these possible interfering agents.

Concerning the DESL pharmaceutical matrix samples, the sensor proved to be selective for DESL compared to the excipients presented in the samples; microcrystalline cellulose, silicon dioxide, magnesium stearate, calcium phosphate, lactose, talc, titanium dioxide and sodium citrate. The excipients were found not to be electroactive on the CMB-MWCNTs/GCE in the tested potential window (0–1.4 V), and the relative DESL responses varied by less than 3.77% in the presence of these compounds.

3.9. Accuracy of the proposed linear sweep voltammetric method

The accuracy of the linear sweep voltammetric method for DESL determination using CMB-MWCNTs/CGE was assessed by comparing the results obtained by the proposed electrochemical sensing method with that of a validated spectrophotometric method [2]. These methods were applied to the analysis of the commercial pharmaceutical preparations containing DESL, and the results are presented in Table 3. Both methods presented concordant results with relative errors less than 4.00%. Taking into account the results of the *F* test [50] presented in Table 3, the calculated *F* values (F_{calc}) were lower than the critical *F* (19.0), meaning that the analytical methods presented equivalent levels of precision. A paired *t*-test [50] was also applied. The calculated *t* value of 2.09 was also lower than the critical *t* value (2.20, 95% of confidence level). The linear sweep voltammetric method was found not to be statistically different when compared to the validated spectrophotometric procedure.

The efficacy of the CMB-MWCNTs/CGE sensor was also evaluated in determining DESL in spiked rat serum. Rat serum was spiked with 50 μmol L^{-1} DESL. An aliquot of 500 μL of spiked serum was directly transferred into the electrochemical cell containing 10 mL of potassium hydrogen-phosphate solution (pH 8.0) and linear sweep voltammograms were recorded. Successive aliquots of DESL standard solutions (5, 10, 15 and 20 μL of 1.0 mmol L^{-1}) were added, and the voltammograms were recorded. An average recovery of 102.6 ± 2.6% indicated the feasibility of the sensoring device in the determination of DESL in this biological sample.

4. Conclusion

In the work reported herein, we constructed a new electrochemical sensoring device by dispersing MWCNTs in aqueous media containing carboxymethylated botryosphaeran. The new fabricated sensor device (CMB-MWCNTs/CGE) was successfully applied to pharmaceutical preparations containing DESL, and the results obtained were statistically similar to those obtained by a validated spectrophotometric method. The results for the determination of DESL in spiked rat serum samples, indicated no interference from the matrix materials, confirming the sensor selectivity in a complex biological sample. Finally, the results confirmed that the CMB-MWCNTs/GCE electrode used in conjunction with the LSV technique presented satisfactory performance in the determination of DESL in pharmaceutical and biological samples. The potential of using CMB in a stabilized MWCNTs aqueous dispersion to fabricate printed (bio)sensors will be a future direction of our work.

Acknowledgements

The authors gratefully acknowledge financial support and scholarships from the Brazilian funding agencies CAPES (grant no. 88882.448537/2019-01 and PROAP 2018), CNPq (grant no. 408591/2018-8; E. R. Sartori), Fundação Araucária do Paraná (grant no. 001/17–3765 E. R. Sartori) and Fundação de Amparo à Pesquisa do Estado de São Paulo (grant no. CEPID/CDMF 2013/07296-2 M. F. S. Teixeira ∴). Special thanks to Laboratório de Microscopia Eletrônica e Microanálise - UEL for SEM imaging, and Dr Dimas A. M. Zaia for access and the use of the spectrophotometer.

Appendix A. Supplementary data

Supplementary data to this article can be found online at https://doi.org/10.1016/j.talanta.2019.120642.

References

[1] M.I. Walash, F. Belal, N. El-Enany, M. Eid, R.N. El-Shaheny, Stability-indicating micelle-enhanced spectrofluorimetric method for determination of loratadine and desloratadine in dosage forms, Luminescence 26 (2011) 670–679, https://doi.org/10.1002/bio.1294.
[2] S.U. Kushare, M. Mali, A. Phatak, P.D. Chaudhari, Spectrophotometric method for simultaneous estimation of desloratadine and pseudoephedrine hydrochloride from tablets and dissolution media, Asian J. Res. Chem. 4 (2011) 1440–1443 ISSN 0974-4169.
[3] M. Qi, P. Wang, Y. Geng, Determination of desloratadine in drug substance and pharmaceutical preparations by liquid chromatography, J. Pharm. Biomed. Anal. 38 (2005) 355–359, https://doi.org/10.1016/j.jpba.2005.01.003.
[4] P. Adamowicz, M. Kała, Simultaneous screening for and determination of 128 date-rape drugs in urine by gas chromatography–electron ionization-mass spectrometry, Forensic Sci. Int. 198 (2010) 39–45, https://doi.org/10.1016/j.forsciint.2010.02.012.
[5] M.M. Aleksić, V.L. Radulović, V.P. Kapetanović, V.M. Savić, The possibility of simultaneous voltammetric determination of desloratadine and 3-hydroxydesloratadine, Acta Chim. Slov. 57 (2010) 686–692 PMID: 24061817 http://www.ncbi.nlm.nih.gov/pubmed/24061817.
[6] D.S. Vidya, M.S. Prasad, M.V. Priya, K. Roja, N. Sreedhar, Voltammetric determination of desloratadine in pharmaceutical and human urine samples using glassy carbon electrode, Int. J. Pharm. Pharm. Sci. 6 (2014) 119–122 https://pdfs.semanticscholar.org/86fe/0e79ef8be179ad9b04f9e766b4927fc3825b.pdf.
[7] V.K. Gupta, R. Jain, K. Radhapyari, N. Jadon, S. Agarwal, Voltammetric techniques for the assay of pharmaceuticals-A review, Anal. Biochem. 408 (2011) 179–196, https://doi.org/10.1016/j.ab.2010.09.027.

[8] T.A. Silva, F.C. Moraes, B.C. Janegitz, O. Fatibello-Filho, Electrochemical biosensors based on nanostructured carbon black: a review, J. Nanomater. 2017 (2017) 1–14, https://doi.org/10.1155/2017/4571614.

[9] N. Yang, S. Yu, J.V. Macpherson, Y. Einaga, H. Zhao, G. Zhao, G.M. Swain, X. Jiang, Conductive diamond: synthesis, properties, and electrochemical applications, Chem. Soc. Rev. 48 (2019) 157–204, https://doi.org/10.1039/C7CS00757D.

[10] L. Bandžuchová, Ľ. Švorc, M. Vojs, M. Marton, P. Michniak, J. Chýlková, Self-assembled sensor based on boron-doped diamond and its application in voltammetric analysis of picloram, Int. J. Environ. Anal. Chem. 94 (2014) 943–953, https://doi.org/10.1080/03067319.2013.879300.

[11] Ľ. Švorc, K. Borovská, K. Cinková, D.M. Stanković, A. Planková, Advanced electrochemical platform for determination of cytostatic drug flutamide in various matrices using a boron-doped diamond electrode, Electrochim. Acta 251 (2017) 621–630, https://doi.org/10.1016/j.electacta.2017.08.077.

[12] J. Svítková, T. Ignat, Ľ. Švorc, J. Labuda, J. Barek, Chemical modification of boron-doped diamond electrodes for applications to biosensors and biosensing, Crit. Rev. Anal. Chem. 46 (2016) 248–256, https://doi.org/10.1080/10408347.2015.1082125.

[13] A. Hajializadeh, S. Jahani, S. Tajik, H. Beitollahi, Electrochemical behavior and determination of carbidopa on modified graphite screen printed electrode, Anal. Bioanal. Electrochem. 10 (2018) 404–413.

[14] H. Beitollahi, F. Movahedifar, S. Tajik, S. Jahani, A review on the effects of introducing CNTs in the modification process of electrochemical sensors, Electroanalysis 30 (2018) 1–10, https://doi.org/10.1002/elan.201800370.

[15] A.J. Bard, Chemical modification of electrodes, J. Chem. Educ. 60 (1983) 302–304.

[16] S. Kumar, V. Vicente-Beckett, Glassy carbon electrodes modified with multiwalled carbon nanotubes for the determination of ascorbic acid by square-wave voltammetry, Beilstein J. Nanotechnol. 3 (2012) 388–396, https://doi.org/10.3762/bjnano.3.45.

[17] J.J. Gooding, Nanostructuring electrodes with carbon nanotubes: a review on electrochemistry and applications for sensing, Electrochim. Acta 50 (2005) 3049–3060, https://doi.org/10.1016/j.electacta.2004.08.052.

[18] J. Scremin, E.C.M. Barbosa, C.A.R. Salamanca-Neto, P.H.C. Camargo, E.R. Sartori, Amperometric determination of ascorbic acid with a glassy carbon electrode modified with TiO2-gold nanoparticles integrated into carbon nanotubes, Microchim. Acta 185 (2018) 251, https://doi.org/10.1007/s00604-018-2785-7.

[19] B. Mokhtari, D. Nematollahi, H. Salehzadeh, Electrochemical simultaneous determination of nifedipine and its main metabolite dehydronifedipine using MWCNT modified glassy carbon electrode, J. Mol. Liq. 264 (2018) 543–549, https://doi.org/10.1016/J.MOLLIQ.2018.05.082.

[20] K. Sipa, M. Brycht, A. Leniart, P. Urbaniak, A. Nosal-Wiercińska, B. Pałecz, S. Skrzypek, β–Cyclodextrins incorporated multi-walled carbon nanotubes modified electrode for the voltammetric determination of the pesticide dichlorophen, Talanta 176 (2018) 625–634, https://doi.org/10.1016/J.TALANTA.2017.07.084.

[21] Y. Zhou, Y. Fang, R. Ramasamy, Non-covalent functionalization of carbon nanotubes for electrochemical biosensor development, Sensors 19 (2019) 392, https://doi.org/10.3390/s19020392.

[22] L. Yang, H. Zhao, C.-P. Li, S. Fan, B. Li, Dual β-cyclodextrin functionalized Au@SiC nanohybrids for the electrochemical determination of tadalafil in the presence of acetonitrile, Biosens. Bioelectron. 64 (2015) 126–130, https://doi.org/10.1016/j.bios.2014.08.068.

[23] T. Rungrotmongkol, U. Arsawang, C. Iamsamai, A. Vongachariya, S.T. Dubas, U. Ruktanonchai, A. Soottitantawat, S. Hannongbua, Increased dispersion and solubility of carbon nanotubes noncovalently modified by the polysaccharide biopolymer, chitosan: MD simulations, Chem. Phys. Lett. 507 (2011) 134–137, https://doi.org/10.1016/J.CPLETT.2011.03.066.

[24] S.M. Fatemi, M. Foroutan, Recent developments concerning the dispersion of carbon nanotubes in surfactant/polymer systems by MD simulation, J. Nanostruct. Chem. 6 (2016) 29–40, https://doi.org/10.1007/s40097-015-0175-9.

[25] R.F.H. Dekker, E.A.I.F. Queiroz, M.A.A. Cunha, A.M. Barbosa-Dekker, Botryosphaeran – a fungal exopolysaccharide of the (1→3)(1→6)-β-D-glucan kind: structure and biological functions, in: E. Cohen, H. Merzendorfer (Eds.), Extracell. Sugar-Based Biopolym. Matrices, Biol. Syst. 12, Springer Nature Switzerland, 2019, pp. 433–484, , https://doi.org/10.1007/978-3-030-12919-4_11.

[26] A.P.P. Eisele, C.F. Valezi, T. Mazziero, R.F.H. Dekker, A.M. Barbosa-Dekker, E.R. Sartori, Layering of a film of carboxymethyl-botryosphaeran onto carbon black as a novel sensitive electrochemical platform on glassy carbon electrodes for the improvement in the simultaneous determination of phenolic compounds, Sens. Actuators B Chem. 287 (2019) 18–26, https://doi.org/10.1016/J.SNB.2019.02.004.

[27] A.M. Barbosa, R.M. Steluti, R.F. Dekker, M.S. Cardoso, M. Corradi da Silva, Structural characterization of Botryosphaeran: a (1→3;1→6)-β-D-glucan produced by the ascomyceteous fungus, Botryosphaeria sp, Carbohydr. Res. 338 (2003) 1691–1698, https://doi.org/10.1016/S0008-6215(03)00240-4.

[28] J. Xu, W. Liu, W. Yao, X. Pang, D. Yin, X. Gao, Carboxymethylation of a polysaccharide extracted from Ganoderma lucidum enhances its antioxidant activities in vitro, Carbohydr. Polym. 78 (2009) 227–234, https://doi.org/10.1016/J.CARBPOL.2009.03.028.

[29] G.L. Long, J.D. Winefordner, Limit of detection a closer look at the IUPAC definition, Anal. Chem. 55 (1983) 712A–724A, https://doi.org/10.1021/ac00258a724.

[30] O.V. Kharissova, B.I. Kharisov, E.G. de Casas Ortiz, Dispersion of carbon nanotubes in water and non-aqueous solvents, RSC Adv. 3 (2013) 24812–24852, https://doi.org/10.1039/c3ra43852j.

[31] J. Dai, R.M.F. Fernandes, O. Regev, E.F. Marques, I. Furó, Dispersing carbon nanotubes in water with amphiphiles: dispersant adsorption, kinetics and bundle size distribution as defining factors, J. Phys. Chem. C 122 (2018) 24386–24393, https://doi.org/10.1021/acs.jpcc.8b06542.

[32] P.G. Karagiannidis, S.A. Hodge, L. Lombardi, F. Tomarchio, N. Decorde, S. Milana, I. Goykhman, Y. Su, S.V. Mesite, D.N. Johnstone, R.K. Leary, P.A. Midgley, N.M. Pugno, F. Torrisi, A.C. Ferrari, Microfluidization of graphite and formulation of graphene-based conductive inks, ACS Nano 11 (2017) 2742–2755, https://doi.org/10.1021/acsnano.6b07735.

[33] D. Sinar, G.K. Knopf, Printed graphene interdigitated capacitive sensors on flexible polyimide substrates, 14th IEEE Int. Conf. Nanotechnol, IEEE, 2014, pp. 538–542, , https://doi.org/10.1109/NANO.2014.6968041.

[34] D.K. Gosser, Cyclic Voltammetry: Simulation and Analysis of Reaction Mechanisms, John Wiley & Sons, Inc., New York, 1993.

[35] O.V. Levin, M.P. Karushev, A.M. Timonov, E.V. Alekseeva, S. Zhang, V.V. Malev, Charge transfer processes on electrodes modified by polymer films of metal complexes with Schiff bases, Electrochim. Acta 109 (2013) 153–161, https://doi.org/10.1016/j.electacta.2013.07.070.

[36] M.E. Orazem, B. Tribollet, 18 model-based graphical methods, electrochem, Impedance Spectrosc, 2008, pp. 353–362, https://doi.org/10.1002/9780470381588.

[37] J.-G. Guan, Y.-Q. Miao, Q.-J. Zhang, Impedimetric biosensors, J. Biosci. Bioeng. 97 (2004) 219–226, https://doi.org/10.1263/jbb.97.219.

[38] A.M. Santos, A. Wong, O. Fatibello-Filho, Simultaneous determination of salbutamol and propranolol in biological fluid samples using an electrochemical sensor based on functionalized-graphene, ionic liquid and silver nanoparticles, J. Electroanal. Chem. 824 (2018) 1–8, https://doi.org/10.1016/j.jelechem.2018.07.018.

[39] A. Lasia, Electrochemical Impedance Spectroscopy and its Applications, first ed., Springer-Verlag New York, New York, 2014, https://doi.org/10.1007/978-1-4614-8933-7.

[40] C. Gouveia-Caridade, C.M.A. Brett, Electrochemical impedance characterization of nafion-coated carbon film resistor electrodes for electroanalysis, Electroanalysis 17 (2005) 549–555, https://doi.org/10.1002/elan.200403127.

[41] C.M.A. Brett, V.A. Alves, D.A. Fungaro, Nafion-coated mercury thin film and glassy carbon electrodes for electroanalysis: characterization by electrochemical impedance, Electroanalysis 13 (2001) 212–218, https://doi.org/10.1002/1521-4109(200103)13:3<212::AID-ELAN212>3.0.CO;2-Z.

[42] Y. Yi, G. Weinberg, M. Prenzel, M. Greiner, S. Heumann, S. Becker, R. Schlögl, Electrochemical corrosion of a glassy carbon electrode, Catal. Today 295 (2017) 32–40, https://doi.org/10.1016/j.cattod.2017.07.013.

[43] Y. Yi, J. Tornow, E. Willinger, M.G. Willinger, C. Ranjan, R. Schlçgl, Electrochemical degradation of multiwall carbon nanotubes at high anodic potential for oxygen evolution in acidic media, Chem. ElectroChem 2 (2015) 1929–1937, https://doi.org/10.1002/celc.201500268.

[44] P. Córdoba-Torres, T.J. Mesquita, R.P. Nogueira, Relationship between the origin of constant-phase element behavior in electrochemical impedance spectroscopy and electrode surface structure, J. Phys. Chem. C 119 (2015) 4136–4147, https://doi.org/10.1021/jp512063f.

[45] C.C. Corrêa, S.A.V. Jannuzzi, M. Santhiago, R.A. Timm, A.L.B. Formiga, L.T. Kubota, Modified electrode using multi-walled carbon nanotubes and a metallopolymer for amperometric detection of l-cysteine, Electrochim. Acta 113 (2013) 332–339, https://doi.org/10.1016/j.electacta.2013.09.050.

[46] C. Gao, Z. Guo, J.H. Liu, X.J. Huang, The new age of carbon nanotubes: an updated review of functionalized carbon nanotubes in electrochemical sensors, Nanoscale 4 (2012) 1948–1963, https://doi.org/10.1039/c2nr11757f.

[47] M. Zheng, F. Gao, Q. Wang, X. Cai, S. Jiang, L. Huang, F. Gao, Electrocatalytical oxidation and sensitive determination of acetaminophen on glassy carbon electrode modified with graphene–chitosan composite, Mater. Sci. Eng. C 33 (2013) 1514–1520, https://doi.org/10.1016/J.MSEC.2012.12.055.

[48] R. Brasca, M.A. Romero, H.C. Goicoechea, A.-M. Kelterer, W.M.F. Fabian, Spectroscopic behavior of loratadine and desloratadine in different aqueous media conditions studied by means of TD-DFT calculations, Spectrochim. Acta Part A Mol. Biomol. Spectrosc. 115 (2013) 250–258, https://doi.org/10.1016/j.saa.2013.06.037.

[49] A.J. Bard, L.R. Faulkner, Electrochemical Methods: Fundamentals and Applications, second ed., John Wiley & Sons, Inc., New York, 2001.

[50] S.L.R. Ellison, V.J. Barwick, T.J.D. Farrant, Practical Statistics for the Analytical Scientist, Royal Society of Chemistry, Cambridge, 2009, https://doi.org/10.1039/9781847559555.